Physical Characteristics of Neoclassical Toroidal Viscosity in Tokamaks for Rotation Control and the Evaluation of Plasma Response

S.A. Sabbagh[1], R.E. Bell[2], T.E. Evans[3], N. Ferraro[3], I.R. Goumiri[4], Y.M. Jeon[5], W.H. Ko[5], Y.S. Park[1], K.C. Shaing[6], Y. Sun[7], J.W. Berkery[1], D.A. Gates[2], S.P. Gerhardt[2], S.H. Hahn[5], S.C. Jardin[2], C.W. Rowley[4], K. Tritz[8]

[1]Department of Applied Physics, Columbia University, New York, NY, USA
[2]Princeton Plasma Physics Laboratory, Princeton University, Princeton, NJ, USA
[3]General Atomics, San Diego, CA, USA
[4]Princeton University, Princeton, NJ, USA
[5]National Fusion Research Institute, Daejeon, Republic of Korea
[6]National Cheng Kung University, Tainan, Taiwan
[7]ASIPP, Hefei Anhui, China
[8]Johns-Hopkins University, Baltimore, MD, USA

E-mail contact of main author: sabbagh@pppl.gov

Abstract. Favorable use of low magnitude ($\delta B/B_0 \sim O(10^{-3})$) three-dimensional (3D) magnetic fields in tokamaks includes mitigation of ELMs and Alfvénic modes, and alteration of the plasma rotation profile, ω_ϕ, to strongly affect the stability of NTMs and RWMs. However, in ITER, these fields can significantly reduce the fusion gain, Q, by increasing alpha particle transport. These effects have been theoretically addressed using neoclassical toroidal viscosity (NTV) theory. NTV magnitude and profile that determines the critical 3D applied field level for Q reduction, or for ω_ϕ feedback control, depends on the field spectrum, plasma collisionality, and plasma response to the field. The present work examines the physical characteristics of NTV with new analysis of results from NSTX and KSTAR. Experimental angular momentum alteration is directly compared quantitatively to theoretical NTV torque density profiles, T_{NTV}, created by a range of applied 3D field spectra and plasma parameters in NSTX including configurations with dominant n = 2 and n = 3 field components. Large radial variations of T_{NTV} are found in ideal MHD models when the flux surface displacement ξ is derived using an assumption of a fully penetrated $\delta\boldsymbol{B}$. In contrast, experimentally measured T_{NTV} does not show strong torque localization. NSTX experiments yield a computed $|\xi| \sim 0.3$cm, smaller than the ion banana width, and averaging T_{NTV} over the banana width more closely matches the measured dL/dt profile. Results from a model-based rotation controller designed and tested using NTV from applied 3D fields as an actuator for instability control are shown. A favorable observation for ω_ϕ control, clearly illustrated by KSTAR experiments, is the lack of hysteresis of ω_ϕ when altered by non-resonant NTV. These experiments also show the theoretical scaling of T_{NTV} with $\delta\boldsymbol{B}^2$ and ion temperature $\sim T_i^{2.5}$. Due to this strong theoretical dependence of the T_{NTV} profile on $\delta\boldsymbol{B}$, the T_{NTV} measurements significantly constrain the allowable field amplification. Plasma response models presently being tested against experiment include the fully-penetrated $\delta\boldsymbol{B}$ model, and various physics models in the M3D-C^1 resistive MHD code. Initial analysis shows that the M3D-C^1 single-fluid model produces a flux surface-averaged $|\delta\boldsymbol{B}|$ consistent with the experimentally measured T_{NTV}.

1. Introduction

Favorable use of low magnitude ($|\delta\boldsymbol{B}|/B_0 \sim O(10^{-3})$) three-dimensional (3D) magnetic fields applied to tokamaks has been demonstrated by the mitigation of ELMs [1] and Alfvenic modes [2], and by altering the plasma rotation profile, ω_ϕ, to maintain stability of disruption-producing modes (e.g. NTMs, RWMs). However, in ITER, these fields can significantly reduce the fusion gain, Q, by increasing alpha particle transport. These effects have been theoretically addressed by using a generalization of neoclassical toroidal viscosity (NTV) theory [3]. A modest level of 3D applied field $\sim 10^{-4}$, near but below the level needed for ELM mitigation in DIII-D, is sufficiently large to negatively impact Q. NTV magnitude and profile that determines the critical 3D applied field level for Q reduction, or for ω_ϕ feedback control, depends on the field spectrum, plasma collisionality, and the plasma response to the field. Expanded, detailed quantitative comparisons of NTV theory to experiment are therefore critical to accurately predict its effects on ITER and other tokamaks.

Data and analysis of dedicated NTV experiments on the National Spherical Torus Experiment (NSTX) are quantitatively compared to theory to examine and compare the expected and observed NTV characteristics. The NTV perturbation experiments allow a unique, quantitative assessment of plasma response modeling – presently a state-of-the-art theoretical research area. Due to the strong theoretical dependence of the NTV torque density profile, $T_{NTV} \propto \delta\boldsymbol{B}^2$, the quantitative T_{NTV} profile measurements and analysis performed in this work can significantly and uniquely constrain modeled plasma-induced amplification magnitudes. Complementary results and analysis of dedicated experiments in the Korea Superconducting Tokamak Advanced Research (KSTAR) device are shown, adding long-pulse aspects of NTV for ω_ϕ control, including the critical question of ω_ϕ hysteresis.

2. Experimental characteristics of NTV and comparison to theory

The NSTX device allows the application of 3D magnetic fields from a set of six toroidally-conforming midplane magnetic coils designed for this purpose (FIG. 1). Applied 3D field configurations with dominant toroidal mode number $n > 1$ are generally non-resonant with significant magnetohydrodynamic (MHD) modes, and have been shown to generate plasma rotation profile alteration by NTV to low values of ω_ϕ without mode locking [4]. The basic characteristics of experimental ω_ϕ alteration show that the NTV torque is radially extended, with a relatively smooth profile, and changes continuously as the applied field is increased. T_{NTV} is not simply an integrated torque applied at the plasma boundary, but is rather a radial profile. As shown from NTV theory [5], T_{NTV} depends linearly on ω_ϕ and in the primary collisionality regime for present large tokamaks, $T_{NTV} \propto T_i^{5/2}$. Therefore, the T_{NTV} profile becomes small at the plasma edge. These aspects are all favorable for use of non-resonant NTV for ω_ϕ control.

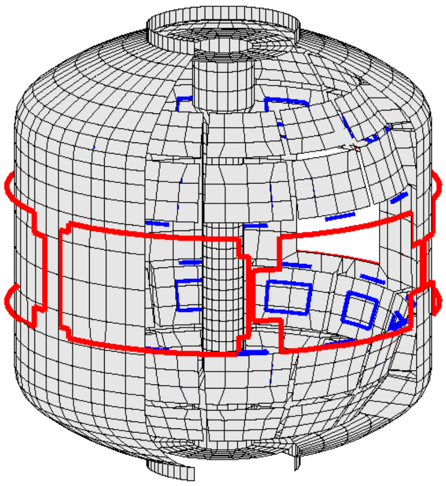

FIG. 1. Cutaway view of NSTX illustrating the midplane 3D coil set (red) mounted on the vacuum vessel.

The T_{NTV} profile can be measured in tokamak experiments by rapidly changing the non-resonant applied 3D field on a timescale significantly faster than the momentum diffusion time, thereby isolating T_{NTV} in the momentum diffusion equation [4]. The power supplies on the NSTX 3D coil system have sufficient bandwidth for this purpose. Experiments utilizing such rapid changes of $\delta\boldsymbol{B}$ best isolate the torque profile. When considering the change in the torque before and after the rapid change in the 3D field, it can be shown that the momentum diffusion equation reduces to the simple equality $-dL/dt = T_{NTV}$, which is applicable until momentum diffusion dissipates the perturbation over a few momentum diffusion times. Here, L is the plasma angular momentum density. The measured change to the plasma angular momentum density profile and the theoretically computed T_{NTV}

profile, created by a range of experimentally applied 3D field spectra and plasma parameters are analyzed, including configurations with dominant n = 2 and n = 3 field components. FIG. 2 compares the theoretically computed T_{NTV} profile components vs. minor radial coordinate ψ_N to the measured change in the plasma angular momentum density, *dL/dt*, as $\delta\boldsymbol{B}$ is rapidly changed. The detailed analysis computes $\delta\boldsymbol{B}$ fully in 3D, and uses the complete Shaing formulation of T_{NTV} valid for all collisionality regimes and the superbanana plateau

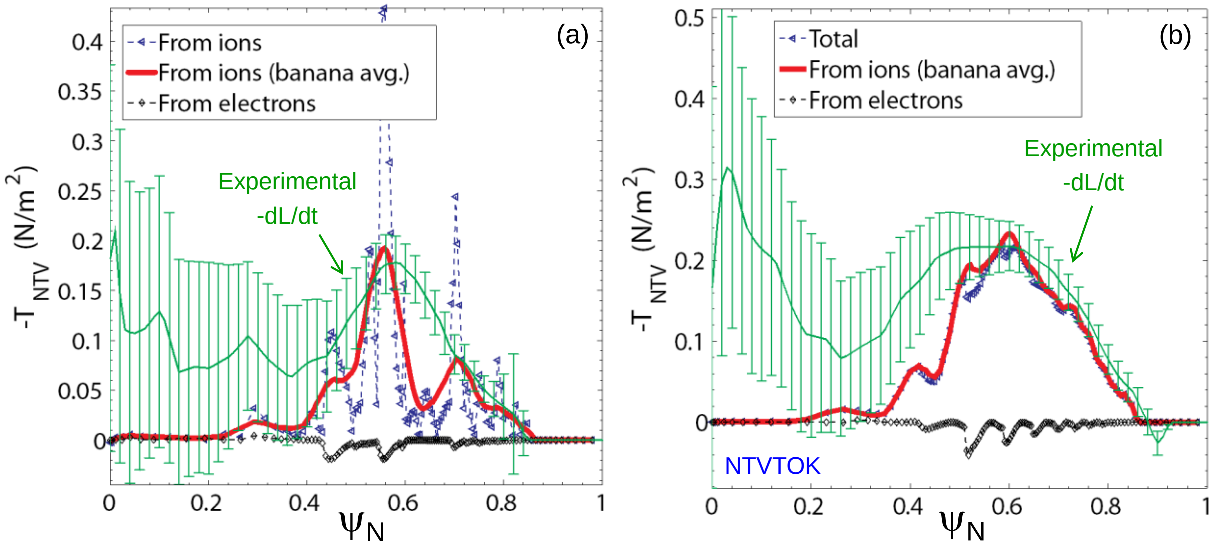

FIG. 2. Theoretical T_{NTV} profile components compared to experiment for (a) an n = 2 applied field configuration in NSTX, computed from (i) ions using the "vacuum field assumption", (ii) ions using banana width-averaging, (iii) electrons, and (b) an n = 3 applied field configuration showing (i) ion component using banana width-averaging (red), (ii) electrons, (iii) total T_{NTV}. The measured (-dL /dt) profile is shown in green.

regime [5] for both ions and electrons as implemented in the NTVTOK code [6]. The calculation includes the effect of flux surface displacement, ξ. A standard decomposition of $\delta\boldsymbol{B}$ into in-surface and normal components is made to first order in the displacement, $\delta B = \vec{b}\bullet\left(\vec{B}/B\right)+\left(\vec{\xi}\bullet\nabla B\right)$, with the analysis shown in FIG. 2 adopting the often-used "vacuum field assumption" to compute ξ [6], in which ξ is computed to be consistent with the fully-penetrated applied 3D vacuum field. As is sometimes shown in recent theoretical publications on NTV, the large radial variations of the theoretical ion T_{NTV} shown in FIG. 2(a) are due in part from this assumption for ξ. In contrast, such large radial variations of T_{NTV} are not observed experimentally. Rather, T_{NTV} is experimentally found to be radially extended, without strong radial localization of the torque as is observed in resonant braking by magnetic islands. Solution of the momentum diffusion equation shows that the charge exchange recombination spectroscopy diagnostic on NSTX could discern details of the ω_ϕ evolution caused by these strong radial variations in certain plasmas analyzed if they existed. Experiments at the low aspect ratio of NSTX yield unique information in this regard as the maximum computed theoretical displacement $|\xi|$ = 0.3cm is smaller than either the ion banana width or gyroradius suggesting that finite-orbit effects will average T_{NTV} over such spatial scales. FIG. 2 shows that averaging the ion T_{NTV} profile over the banana width more closely matches the measured *dL/dt* profile. Note that this measured profile is plotted in MKS units. The theoretically computed T_{NTV} profile utilizes experimental equilibrium reconstructions and associated measurements, and for the illustration, the profiles are scaled (the scale factor, S_f, defined as the ratio of the peak value of *dL/dt* to the peak in T_{NTV} are 1.7 and 0.6 for case (a) and (b) respectively). The error bars shown for the experimental *dL/dt* profile reflect the uncertainty in both the plasma rotation and the measured plasma moment of inertia. The large error bars in the core of the plasma are dominated by the uncertainty in the change of the measured plasma mass. Typically, a change in L is not found outside of the error in the core of the plasma for analysis intervals much less than the momentum diffusion time. In contrast, analysis at times longer than the momentum diffusion time clearly shows the effects of the momentum diffusion of the NTV toward the core region, which spoils the T_{NTV} measurement.

3. Key aspects of NTV for rotation profile control

The stability of disruption-inducing MHD modes in tokamak plasmas, such as neoclassical tearing modes and resistive wall modes depends on the plasma rotation and its profile [7,8]. Control of the plasma rotation profile is a relatively untapped opportunity to enhance disruption avoidance in tokamaks. Rotation control has been successfully produced by closed-loop alteration of injected neutral beam power in DIII-D [9], but has the disadvantages fairly large, discrete steps in momentum input unless high frequency modulation is used (stressing the ion sources) and actuator lag associated with the beam slowing-down time. Non-resonant NTV can also be used to alter the plasma rotation profile without leading to mode locking, since it produces a change in the plasma rotation profile proportional to the rotation velocity. It also allows finer control of the rotation speed compared to NBI since the induced drag torque depends on the square of a continuously variable actuator, the applied field current. Devices with uni-directional neutral beam injection such as NSTX and KSTAR have effectively utilized non-resonant NTV for pre-programmed, open-loop plasma control used in a variety of experiments [4,10-12]. A logical next-step is to use non-resonant NTV as an actuator for real-time, closed-loop rotation control. Understanding the dependence of NTV on the key plasma parameters that typically change during control is critical for the successful use of NTV in either pre-programmed or closed-loop feedback. Potential non-linearities, or possible hysteresis due to variations of NTV as the plasma traverses the operating space of a given tokamak are also key considerations.

3.1. Experimental aspects of NTV for rotation profile control

A dedicated set of experiments have been run on the KSTAR superconducting tokamak which have examined key aspects of NTV when used for plasma rotation control. The results show strong non-resonant $n = 2$ NTV magnetic braking in KSTAR, reducing the plasma rotation to as low as 40% of the maximum value run in these high performance plasmas. The rotation profile pedestal is reduced, altering ω_ϕ toward an L-mode profile shape while maintaining H-mode energy confinement. Analysis of these experiments finds the expected theoretical scaling of T_{NTV} with $\delta\boldsymbol{B}^2$ and strong dependence on ion temperature ($\sim T_i^{2.5}$) [12] compatible with the "1/ν" regime of NTV theory [13]. These experiments have also conclusively demonstrated the important and favorable observation for rotation profile control - a lack of hysteresis on the ω_ϕ profile when altering the rotation by non-resonant NTV, as the profiles reach the same steady-state profile for a given applied 3D field independent of the initial ω_ϕ. This is illustrated in FIG. 3, which shows two long-pulse plasmas, one in which the 3D applied field is stepped up in time, and one in which it is stepped down in time. In both cases, the duration of the step is significantly greater than the momentum diffusion time (by at least a factor of 10), which allows the plasma toroidal rotation profile ample time to settle into a steady-state after each change to the 3D applied field magnitude. In the shot indicated by the solid lines, rotation is monotonically decreased at each step. In the shot indicated by the dashed lines, the rotation is first decreased to the minimum of the series of 3D field steps, and then increases in magnitude as the 3D field is decreased from the initial maximum value taken

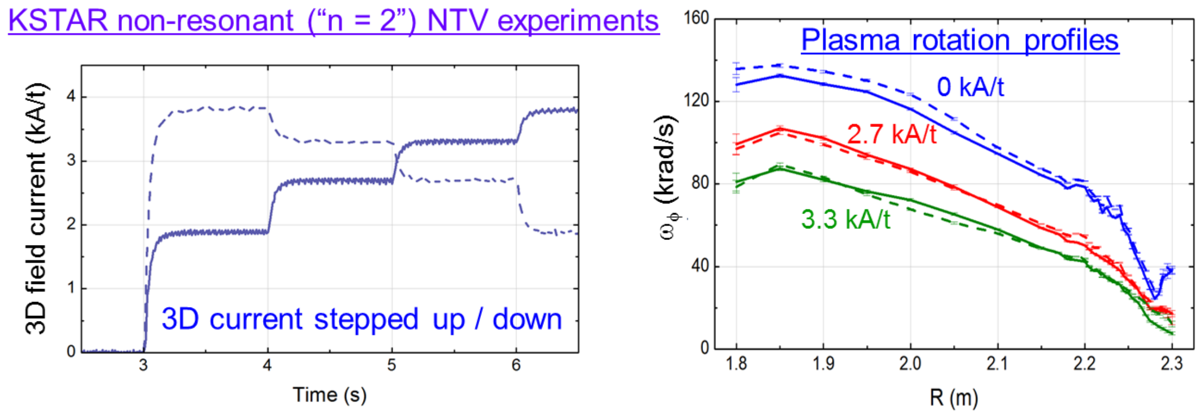

FIG. 3. (left) 3D field current in the In-Vessel Control Coils (IVCC), showing clear increase and decrease in current, taken in steps, and (right) resultant plasma toroidal rotation profiles are shown to be the same for a given level of applied 3D field current, regardless of whether the rotation is slowing, or increasing toward these steady-state profiles.

in the first step. Regardless of whether rotation is increasing or decreasing – as will naturally occur repeatedly in a plasma rotation controller with an NTV actuator – the steady-state rotation profile is the same at each level of the applied 3D field current. This substantially increases confidence that the planned non-resonant NTV actuation will allow successful plasma rotation control in KSTAR and the coming upgrade of NSTX (NSTX-U [14]) with closed-loop feedback. This favorably contrasts JET results that indicated hysteresis in the plasma toroidal rotation evolution when comparing the interval of rotation braking to rotation spin-up as the applied non-axisymmetric field current was increased, then decreased. However the data shown had not reached a steady-state at each value of the applied field shown [15].

3.2. Rotation feedback controller using NTV as an actuator

A model-based, state-space rotation controller designed and tested using NTV torque by applied 3D fields as an actuator has been written and tested. When applied to the solution of the momentum diffusion equation, the controller illustrates the action of the NTV on the time-evolved ω_ϕ profile to be used for instability control. The NSTX-U rotation feedback controller will use six neutral beam sources and for the first time NTV-induced torque as actuators. The controller uses the momentum force balance equation to evolve the plasma rotation frequency which is decomposed into Bessel function states. The model for the NTV torque was developed from a substantial database of NSTX experimental results and the related theoretical analysis as shown in Section 2, simplified to the expression $T_{NTV-c} \propto K \times f\left(n_{e,i}{}^{K1} T_{e,i}{}^{K2}\right) g\left(\delta B(\rho)\right)\left[I_{3Dcoil}{}^{2} \omega_\phi\right]$, where K, $K1$, $K2$ are constants, $n_{e,i}$, $T_{e,i}$ are electron and ion plasma densities and temperatures, g is the radial profile of T_{NTV} generated by the 3D field, and I_{3Dcoil} is the current generating the 3D field. Two illustrative examples of this model and controller are shown in FIG. 4. The left-hand panel shows an open-loop comparison of the rotation controller qualitatively reproducing the plasma rotation evolution

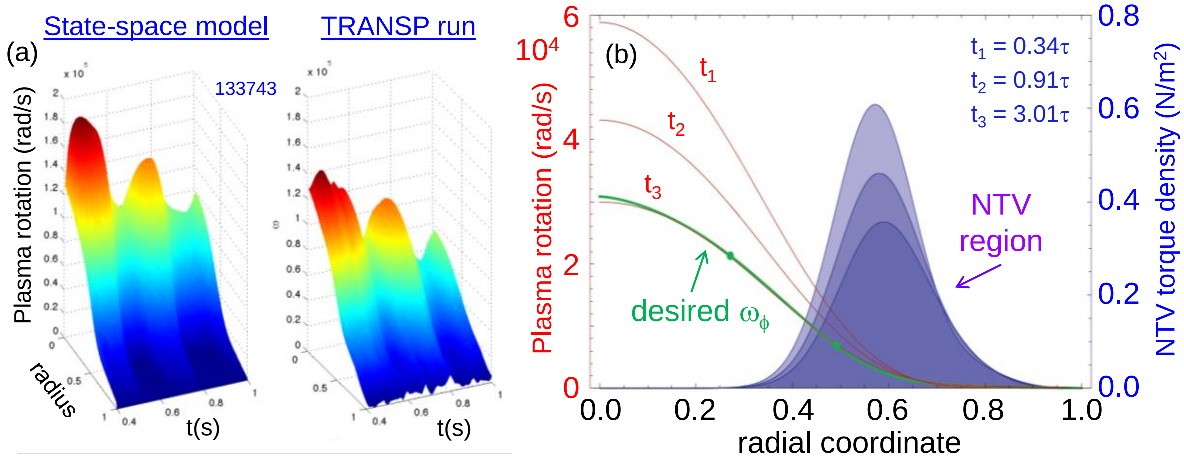

FIG. 4. (a) open-loop plasma rotation evolution of the state-space ω_φ controller model (left) compared to the ω_φ evolution as generated by TRANSP, and (b) ω_φ closed-loop control with NTV as an actuator, showing the $T_{NTV\text{-}c}$ profile and the evolution of ω_φ to the desired target profile.

of a TRANSP code reconstruction of NSTX shot 133743. The right-hand panel of the same figure shows a closed-loop feedback simulation using the rotation controller to match a target plasma toroidal rotation profile by applying an $n = 3$ field configuration to the plasma using the NSTX 3D field coils shown in FIG. 1. The control output is the needed current in the 3D field coils to produce a desired plasma rotation profile. This desired profile is shown in green, and the time evolution of the rotation profiles toward this target profile is shown by three discrete rotation profiles labelled t_1 through t_3, normalized to the momentum diffusion time, τ. Both the strength and the radial profiles of the $n = 3$ NTV torque density are shown in this figure as well at each of these times. As shown, the desired rotation profile is reached in a time of approximately 3τ, since in this case, the action of the NTV torque occurs directly in the outer region of the plasma, then mostly relies on momentum diffusion to alter the rotation

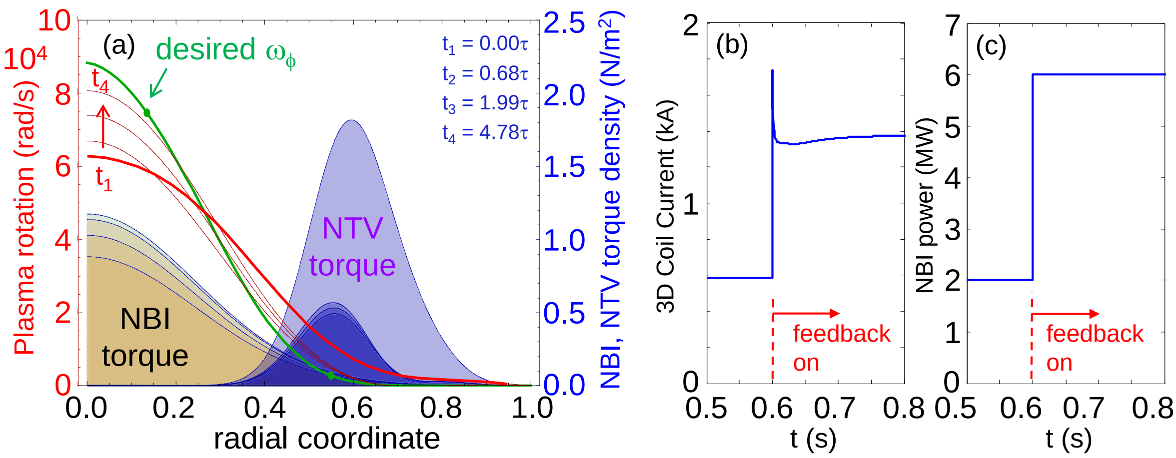

FIG. 5. Plasma rotation controller with NBI and NTV as actuators: (a) evolution of NBI and NTV torque profiles, and ω_φ toward the target profile, (b) 3D coil current, and (c) NBI power evolution.

profile in the core to reach the target rotation profile. More rapid alteration of ω_ϕ in the core and more generalized ω_ϕ profile alteration can be affected by combining NBI and NTV actuators. Results from this addition to the controller are shown in FIG. 5. In this case, the desired ω_ϕ profile has greater peaking with higher core ω_ϕ.The addition of the NBI actuator allows the increased core ω_ϕ, but the desired reduction of ω_ϕ in the outer part of the plasma requires greater T_{NTV} not only to drive the rotation lower, but also to create a larger steady-state NTV torque to balance the increased momentum input from the increased NBI power. The steady-state ω_ϕ is reached in a period less than 5 τ.

4. Utility of NTV experiments and analysis to assess plasma response models

A related critical and advanced area of research regarding T_{NTV} profile computation is the evaluation of the plasma response. A major issue is that the full plasma displacement $\boldsymbol{\xi}$ and its plasma-induced amplification are not directly measured in detail in any experiment and the development of first-principles models is still an active research area. An accurate, first-principles physics model of plasma response has been elusive. The NSTX NTV experimental data and analysis (e.g. as shown in FIG. 2) provides a strong constraint to validate plasma response models of the applied 3D vacuum field across the plasma minor radius. Since T_{NTV} scales as $\delta\boldsymbol{B}^2$, error in any particular theory of plasma response is strongly amplified when compared to the experimentally measured T_{NTV} profile. Models tested against experiment using the comparison of the measured T_{NTV} profile as a figure of merit include the vacuum field assumption for $\boldsymbol{\xi}$ (as stated in Section 2), and various physics models in the M3D-C^1 resistive MHD code, including the single, and two-fluid models.

The analysis given in Section 2 for the theoretical calculation of T_{NTV} using the "vacuum field assumption" to define $\boldsymbol{\xi}$ shows that this relatively simple model well-describes quantitatively the measured T_{NTV} from the NSTX NTV experiments analyzed to date when ion banana width averaging is implemented for the ion component of T_{NTV}. Compiling results from both $n = 2$ and $n = 3$ field configuration experiments yield an average scale factor S_f close to unity, with the largest deviations within 75% of this value. To clarify the significance of this result, note that the calculation assumes that the plasma response displacement $\boldsymbol{\xi}$ is defined to be consistent with the applied 3D field with no additional amplification of this field. So, while there is a plasma response from this field, it does not require a strong amplification of the applied field to be consistent with the experimentally measured T_{NTV}. Specifically, to match a T_{NTV} magnitude that is 75% larger than the experiment would limit the field amplification to the square root of this value, or a factor of 1.32, which is small compared to resonant field amplification magnitudes measured for $n = 1$ fields at high plasma beta in NSTX [10] where these experiments were conducted. This result might be explained by the smaller resonant field amplification measured for the non-resonant $n = 2$ and $n = 3$ field configurations. Note that the NSTX NTV experimental database has not yet been fully analyzed, and consideration of the full database may yet alter this conclusion. Analyses to date using M3D-C^1 show that the single-fluid model produces a flux surface-averaged $\delta\boldsymbol{B}$ magnitude consistent with the experimentally measured T_{NTV} profile in the region of the plasma where T_{NTV} is strongest . In FIG. 6, the surface averaged $\delta\boldsymbol{B}$ field profile from M3D-C^1 is compared to the equivalent profile used in the NTVTOK code calculations of the NTV torque density profile as shown in FIG. 2(a). As FIG. 6 shows, good agreement is found when comparing the single fluid M3D-C^1 field profile and that used to model the instantaneous NTV torque profile using the NTVTOK code in the radial region between $0.5 < \psi_N^{1/2} < 0.9$ using the banana width-averaged model for the NSTX plasma analyzed in FIG. 2. Conclusions regarding the strength of the field perturbation can only be drawn inside this region (at lower ψ_N), since outside of this region the instantaneous NTV torque density measurements made in the experiment are too weak to determine $\delta\boldsymbol{B}$. This is expected, since the T_{NTV} profile scales with ω_ϕ and T_i approximately as $\omega_\phi T_i^{2.5}$ in the operational regime of this plasma, and outside of $\psi_N = 0.9$, both ω_ϕ and T_i are low. In this case, the M3D-C[1] simulation has a core mode, which may be contributing to a larger averaged $\delta\boldsymbol{B}$ in the core region than the NTVTOK calculation shows (dashed red line in FIG. 6). In contrast, the plasma response as computed by the M3D-C[1] two-fluid model presently overestimates the averaged $\delta\boldsymbol{B}$ field profile.

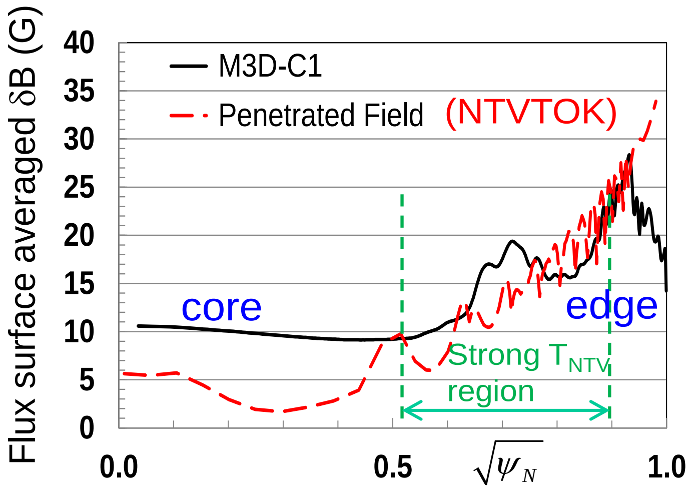

FIG. 6. Flux surface averaged $\delta\boldsymbol{B}$ from a single fluid M3D-C[1] simulation (solid black) and NTVTOK (dashed red) used to calculate T_{NTV} for the n = 3 applied field configuration as shown in FIG. 2.

This research was supported by the U.S. Department of Energy under contracts DE-FG02-99ER54524 and DE-AC02-09CH11466.

---

[1] EVANS, T.E., MOYER, R.A., BURRELL, K.H., et al., Nature Physics **2** (2006) 419.

[2] BORTOLON, A., HEIDBRINK, W.W., KRAMER, G.J, et al., Phys. Rev. Lett. **110** (2013) 265008.

[3] SHAING, K.C. and HSU, C.T., Nucl. Fusion **54** (2014) 033012.

[4] ZHU, W., SABBAGH, S.A., BELL, R.E., et al., Phys. Rev. Lett. **96** (2006) 225002.

[5] SHAING, K.C., SABBAGH, S. A., and CHU, M. S., Nucl. Fusion **50** (2010) 025022.

[6] SUN, Y., LIANG Y., SHAING, K.C., et al., Nucl. Fusion **51** (2011) 053015.

[7] GERHARDT, S.P., BRENNAN, D.P., BUTTERY, R., et al 2009 Nucl. Fusion **49** (2009) 032003.

[8] BERKERY, J.W., SABBAGH, S.A., BETTI, R., et al., Phys. Rev. Lett. **104** (2010) 035003.

[9] SCOVILLE, J.T., HUMPHREYS, D.A., FERRON, J.R., et al., Fusion Eng. and Design **82** (2007) 1045.

[10] SABBAGH, S.A. BERKERY, J.W., BELL, R.E., et al., Nucl. Fusion **50** (2010) 025020.

[11] PARK, Y.S., SABBAGH, S.A., BIALEK, J.M., et al. Nucl. Fusion **53** (2013) 083029.

[12] PARK, Y.S., SABBAGH, S.A., KO, W.H., et al., “Plasma Rotation Alteration by Non-axisymmetric Magnetic Fields, Resistive MHD Stability Analysis, and High Normalized Beta Plasmas Exceeding the Ideal Stability Limit in KSTAR”, IAEA Fusion Energy Conference (2014) paper EX/P8-5.

[13] SHAING, K.C., Phys. Plasmas **10** (2003) 1443.

[14] ONO, M., CHRZANOWSKI, J., DUDEK, L., et al., “Progress toward commissioning and plasma operation in NSTX-U”, IAEA Fusion Energy Conference (2014) paper FIP/P8-30.

[15] LIANG, Y., KOSLOWSKI, H. R., THOMAS, P. R., et al. Nucl. Fusion **50** (2010) 025013.